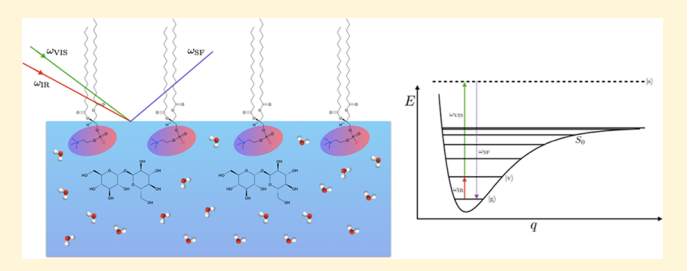


Cooperative Adsorption of Trehalose to DPPC Monolayers at the Water—Air Interface Studied with Vibrational Sum Frequency Generation

Katie A. Link,[†] Gabrielle N. Spurzem,[†] Aashish Tuladhar,[§] Zizwe Chase, ^{||} Zheming Wang, [§] Hongfei Wang, ¹ and Robert A. Walker*, [†], [‡]

Supporting Information

ABSTRACT: A combination of surface tension, surfacespecific vibrational spectroscopy, and differential scanning calorimetry experiments was performed to examine the ability of lipid films to enrich interfacial organic content by attracting soluble, neutral saccharides from bulk aqueous solution. This "cooperative adsorption" hypothesis has been proposed as a possible source of the high organic fractions found in sea spray aerosols and is believed to be responsible for cryoprotection in some organisms. Experiments described in this work show



that the neutral disaccharide trehalose (Tre) is drawn to lipid films composed of dipalmitoylphosphatidylcholine (DPPC), a saturated lipid that is a major component of most eukaryotic cells. The effects of Tre on DPPC monolayer structure and organization were tested with tightly packed monolayers in the two-dimensional solid phase (40 Å²/molecule) and more expanded monolayers in the two-dimensional liquid condensed phase (55 $Å^2$ /molecule). Surface tension data show that DPPC monolayer behavior remains largely unchanged until Tre bulk concentrations are sufficiently high (>50 mM). In contrast, surface-specific vibrational sum frequency spectra show that when Tre bulk concentrations are ≥10 mM, DPPC monolayers in their liquid condensed state (55 Å²/molecule) became more ordered, implying relatively strong noncovalent interactions between the two species. Tre also induces changes in DPPC bilayer behavior as evidenced by a gel-to-liquid crystalline phase transition temperature that increases with increasing Tre concentration. This result suggests that Tre associates with the DPPC headgroups in very specific ways leading to partial dehydration. Together, these results support the cooperative adsorption mechanism under some circumstances, namely, that there is a minimum aqueous phase Tre concentration required to induce observable structural changes in a lipid monolayer and that these effects are most pronounced with DPPC monolayers in their liquid condensed state compared to those of a tightly packed two-dimensional solid.

INTRODUCTION

Lipid film interactions with small molecules such as carbohydrates and synthetic organics continue to attract attention due to the link between these associations and biological and environmental processes.¹⁻⁴ Cell membranes are primarily composed of lipids, and the interaction between these lipids and small molecules controls membrane permeability to drugs and pesticides. Lipids are also a major component of lung surfactant; so, identifying how airborne environmental contaminants interact with the lipid films is essential for predicting the biological consequences of pollution and understanding the origins and treatments of lung diseases including emphysema and cancer.5-

Instrumental investigations into interactions between lipids and insoluble small molecules have provided valuable insight into the condensing effect molecules such as cholesterol can have on lipid monolayers.^{9,10} Insoluble small molecules can interact in a different manner with lipid monolayers. The interaction of these small, water-soluble molecules, including carbohydrates and many pesticides with membrane interfaces, will arise from a subtle competition between solvation forces in bulk solution and noncovalent interactions between the solute

Received: August 14, 2019 Revised: September 24, 2019 Published: September 25, 2019

[†]Department of Chemistry and Biochemistry and [‡]Montana Materials Science Program, Montana State University, Bozeman, Montana 59717, United States

[§]Physical Sciences Division, Physical and Computational Sciences Directorate, Pacific Northwest National Laboratory, Richland, Washington 99352, United States

Department of Physics and Astronomy, Howard University, Washington, D.C. 20059, United States

 $^{^\}perp$ Department of Chemistry and Shanghai Key Laboratory of Molecular Catalysis and Innovative Materials, Fudan University, Shanghai 200433, China

The Journal of Physical Chemistry B

and a lipid film. If the small organic molecules are charged, attractive Coulomb forces are likely to drive cooperative adsorption much in the same way that divalent cations such as Mg²⁺ and Zn²⁺ are known to associate with negatively charged lipid headgroups and induce lipid monolayer condensation.^{11–13} Cooperative adsorption has also been inferred for negatively and positively charged carbohydrates that have had significant effects on lipid film organization.^{14–16} In systems with larger, neutral molecules, such as certain polysaccharides, interactions between lipid films and the organic solutes will necessarily be limited to hydrogen bonding and general dipolar attraction.

Saccharide association with lipid membranes is particularly important given the ability of some saccharides to protect membrane structure in environmentally hostile conditions. Specifically, organisms have been able to remain viable under dehydrating conditions by accumulating large concentrations of saccharides in the cell membrane.³ One notable saccharide that contributes to this phenomenon is trehalose, a disaccharide composed of two glucose molecules that has been identified as an effective cryoprotectant ^{17,18} (Figure 1). Trehalose, with

Figure 1. Molecular structures of the phospholipid, dipalmitoylphosphatidylcholine (DPPC) (top), and the disaccharide, trehalose (bottom).

concentrations as low as 0.1 g Tre/g lipid, prevents adjacent membranes from fusing when dehydrated.¹⁷ At higher Tre concentrations, 1 g Tre/g lipid, water-soluble vesicle contents are prevented from leaking out during rehydration.¹⁷ While the effects of Tre on membrane integrity are clear, the debate continues regarding the mechanism(s) responsible for the Tre's protective effects.

Experimental studies of Tre with membranes have focused on elucidating Tre's bioprotective mechanisms using techniques including NMR, ¹⁹ differential scanning calorimetry (DSC), ²⁰⁻²² and Fourier transform infrared (FTIR). ²³⁻²⁵ Several hypotheses have been advanced to explain the experimental and computational results of how Tre interacts with lipids and the water around the lipid membranes. For example, the water replacement hypothesis proposes that the saccharides replace water molecules near the lipid by forming Hbonds with the charged groups at the membrane surface. 3,26 Alternatively, the water entrapment hypothesis suggests that the saccharides concentrate water near the membrane and preserve lipid headgroup hydration shells. 3,26 The vitrification hypothesis states that adsorbed Tre forms an amorphous glass that reduces mechanical disruption in membranes.^{3,26} The hydration forces hypothesis requires that Tre molecules are excluded from the surface, indirectly reducing the compressive stress in membranes during dehydration. The headgroup-bridging hypothesis is an

extension of the water replacement hypothesis, in which the sugars hydrogen-bond with multiple lipid headgroups forming a scaffold.³ Many researchers have acknowledged that a combination of these mechanisms likely work in tandem to keep the membrane hydrated during times of osmotic or thermal stress.^{3,26} Of these mechanisms, MD simulations typically point to the water replacement and H-bond bridging as being most important, but characteristics of all of the above mechanisms can occur in simulations, leaving considerable ambiguity about this process.

An important point to note is that very little work has considered Tre—lipid interactions under conditions likely to be found in natural settings, namely, with fully hydrated lipid monolayers/bilayers in a solution of relatively dilute Tre. Under these circumstances, the lipid film will have to attract Tre from solution, enriching Tre content at the film surface through some sort of cooperative adsorption mechanism. Alternatively, if the cell is synthesizing its own Tre in response to environmental stress, noncovalent interactions will have to keep saccharides cooperatively adsorbed to the membrane surface so that they do not diffuse into the solution.

Studies described below test whether cooperative adsorption will draw Tre from aqueous solutions to a DPPC monolayer adsorbed to an aqueous-vapor interface. Unlike previous cooperative adsorption studies that featured the charged monosaccharides, glucosamine (cationic) and glucuronic acid (anionic), 14-16 this report focuses on Tre, an uncharged disaccharide. Our examination includes both surface tension measurements and surface-specific, nonlinear optical vibrational experiments. Together, results strongly suggest that cooperative adsorption does enhance interfacial Tre concentrations and that adsorbed Tre promotes organization within the DPPC film. These effects become less pronounced with DPPC monolayers that are already tightly packed. To explore these interactions further, DSC measurements show that Tre affects lipid membrane properties when the Tre concentrations are ≥ 50 mM. Langmuir isotherms show little change in surface tension with Tre below this concentration. DSC measurements were not performed below this 50 mM threshold, but the DSC data do show the growth of a low-temperature shoulder with increasing Tre concentrations. DPPC monolayer features in vibrational sum frequency generation (VSFG) measurements show higher sensitivity to lower Tre concentrations with a strong increase in methyl group vibrational intensity with only 10 mM Tre in the subphase. These results support a cooperative adsorption mechanism where Tre interacts noncovalently with the monolayer, inducing greater order among the acyl chains. These findings together with literature reports imply that hydrogen bonding is likely responsible for cooperative adsorption, but measurements in this work do not decisively identify whether this H-bonding occurs with headgroups or the lipid's 3-carbon glycero backbone.

EXPERIMENTAL SECTION

1,2-Dimyristoyl-sn-glycero-3-phosphocholine (DPPC, powder, >99%) was purchased from Avanti Polar Lipids Inc. (Alabaster, Alabama). D-(+)-Trehalose dihydrate from starch (Tre, powder, \geq 99%) was purchased from Sigma-Aldrich (St. Louis, MO). HPLC-grade chloroform (99.9%) was purchased from Fisher Scientific. All chemicals were used without further purification. Millipore water (resistivity of 18.2 M Ω) was used for all aqueous sample preparations. Structures for these two molecules, DPPC and Tre, are shown in Figure 1.

Preparation of Samples. DPPC lipid stock solutions (0.7 mg/mL) were prepared in chloroform and sonicated for 10 min. Aqueous samples for VSFG measurements were prepared in borosilicate Petri dishes. These Petri dishes were acid-washed (50/50 vol nitric/sulfuric) and rinsed with Millipore water before use. The DPPC/chloroform stock solution was spread on each subphase with a Hamilton glass microsyringe.

Vibrational Sum Frequency Generation. Vibrational sum frequency generation (VSFG) is a second-order nonlinear spectroscopy technique. Within the electric dipole approximation, only Raman- and IR-active vibrational transitions that are in a noncentrosymmetric environment can produce an SFG response. This specificity allows molecules at the surface to be studied without contributions from bulk solution species. To perform VSFG experiments, two incident laser sources, a tunable IR source and a fixed 800 nm visible source, are overlapped in space and time at a surface. This condition creates a coherent nonlinear polarization, producing an SFG response at the sum of the two input frequencies. When the IR source is resonant with a vibrational mode of a species at the surface, the SF signal can be resonantly enhanced.

In sum frequency generation experiments, the intensity of the resultant SF signal, $I(\omega)$, is proportional to the square of the effective portion of the second-order nonlinear susceptibility, $\chi_{\rm eff}^{(2)}$ (eq 1). The $\chi_{\rm eff}^{(2)}$ is made up of a nonresonant part, $\chi_{\rm NR,eff}^{(2)}$ and a resonantly enhanced part, $\chi_{\rm q,eff}^{(2)}$. The resonantly enhanced part depends on resonant frequency, ω_q , and the damping constant of the qth vibrational mode, Γ_q (eq 2). Recent reports in the VSFG literature have shown that at charged aqueous interfaces, the static, surface potential, $\Phi(0)$, can lead to changes in the VSFG intensity and line shape (eq 3). Physical Popular Po

$$I(\omega) \propto |\chi_{\text{eff}}^{(2)}|^2$$
 (1)

$$|\chi_{\text{eff}}^{(2)}|^2 = \left|\chi_{\text{NR,eff}}^{(2)} + \sum_{q, \text{eff}} \frac{\chi_{q, \text{eff}}^{(2)}}{\omega_{\text{IR}} - \omega_q + i\Gamma_q}\right|$$
 (2)

$$I(\omega) \propto \left| \chi_{\rm NR}^{(2)} + \sum \frac{\chi_{q, \rm eff}^{(2)}}{\omega_{\rm IR} - \omega_q + i\Gamma_q} + (\chi_1^{(3)} + i\chi_2^{(3)}) \Phi(0) \right|$$
(3)

While several studies have shown that $\chi^{(3)}$ can affect VSFG spectra in substantive and nonintuitive ways, $^{29-36}$ many of these treatments assume an ideal electric double layer whose extent into solution depends on aqueous phase ionic strength. In cases where a classical double-layer description does not apply, $\chi^{(3)}$'s importance is diminished. For the experiments in this work, contributions from a simple $\chi^{(2)}$ response, as well as contributions from the static, electric-field-induced $\chi^{(3)}$ effect, were considered. In our analysis, we found that fitting data and including $\chi^{(3)}$ effects led only to very small predicted changes in intensities, line shapes, and band positions in the C–H stretching region (2800–3000 cm⁻¹). The calculations without surface potential contributions showed no asymmetric broadening in the peak shape, shifting of the band peak position, or asymmetric intensity increasing/decreasing—all observations consistent with the data acquired in our studies. Thus, the data and analysis presented below reflect only $\chi^{(2)}$ contributions.

VSFG spectra were acquired in three different polarization conditions, SSP, PPP, and SPS (listed in order of sum, visible, and IR polarizations, respectively). SPS and SSP polarization combinations sample a single $\chi^{(2)}$ element, while the PPP polarization combination samples all nonzero $\chi^{(2)}$ elements. The SSP polarization combination was the primary polarization combination used to assess the effects of Tre adsorption on DPPC structure and organization.

The VSFG setup at Montana State University has been described in detail elsewhere. Briefly, this system uses a Coherent Libra Ti:sapphire laser with an 85 fs pulse and a 1 kHz repetition rate, which produces 3.3 W of 800 nm light. An 80/20 beam splitter reflects 80% of the light into a Coherent OPerA Solo optical parametric amplifier to produce IR light. The 800 nm light and the IR light (centered at ~3.4 μ m) are focused onto the sample at 48 and 38°, respectively, from surface normal. The SF response is collimated and isolated before being focused into a monochromator (SpectraPro-300i, Acton Research Corporation) and then dispersing onto a 1340 \times 100 pixel CCD (PIXIS100B, Princeton Instruments). For vibrational resonances in the 3.4 μ m region, the assembly has a spectral resolution of $<10~{\rm cm}^{-1}$.

Surface Tension. Surface tension measurements were carried out using methods described previously. ¹⁴ Briefly, a NIMA Langmuir trough (Model 302LL) equipped with an NIMA PS4 pressure sensor and a micro processor interface 104 was used to perform measurements. Paper Wilhelmy plates (Brown Waite Engineering) were used to measure surface tension. The Langmuir trough barriers were closed at a speed of 10 cm²/min.

Surface pressure (π) was measured as a function of surface area. The surface pressure is related to the surface tension of the underlying neat liquid phase (γ_0) and the surface tension that results from both the subphase and the surfactant monolayer (γ) as shown in eq 4

$$\Pi = \gamma_0 - \gamma \tag{4}$$

Excess free energy of mixing, $\Delta G_{\rm mix}^{\rm E}$, can be calculated for ideal mixed monolayers containing two species that are restricted to the surface (eq 5). In eq 5, A_{12} is the actual area per molecule of a mixed monolayer, A_1 and A_2 are the area per molecule of a pure monolayer of one of the species in the mixed monolayer, and x_1 and x_2 are the mole fractions of each of the species in the mixed monolayer 37,38

$$\Delta G_{\text{mix}}^{\text{E}} = \int_{\pi_1}^{\pi_2} N_{\text{A}} (A_{12} - x_1 A_1 - x_2 A_2) d\pi$$
 (5)

This equation can be simplified further. We assume that DPPC (species 1) is the only species constrained to the aqueous/vapor interface because trehalose is highly soluble in aqueous solution (69 g Tre per 100 g $\rm H_2O$ at 20 °C or ~1.8 M). With this assumption, eq 5 becomes

$$\Delta G_{\text{mix}}^{\text{E}} = \int_{\pi_1}^{\pi_2} N_{\text{A}} (A_{12} - A_1) d\pi$$
 (6)

Differential Scanning Calorimetry. Differential scanning calorimetry (DSC) measurements were made using a TA Instruments Discovery (New Castle, DE). Vesicle solutions were put into Tzero pans with Tzero hermetic lids (TA Instruments) and sealed. Each sample was equilibrated to 20 $^{\circ}$ C before heating by 0.5 $^{\circ}$ C/min until 55 $^{\circ}$ C to capture the transition temperature $T_{\rm m}$ of DPPC at approximately 41 $^{\circ}$ C.

Vesicle solutions were made using standard protocols. Briefly, a \sim 1 mg/mL solution of DPPC in chloroform in a round-bottom flask was dried with a rotary evaporator with a bath temperature set to \sim 10 °C greater than $T_{\rm m}$ of DPPC. This procedure resulted in a lipid film that was then rehydrated with Millipore water (pH 5.9) and sonicated for 20 min in a bath of \sim 10 °C greater than the $T_{\rm m}$. This vesicle solution was then mixed with trehalose solutions to create a 10 mM DPPC vesicle solution containing the desired amount of trehalose. These solutions were allowed to equilibrate for at least 20 min before use.

■ RESULTS AND DISCUSSION

Trehalose is highly soluble in water. However, this solubility does not exclude Tre from being present at the surface. Figure 2

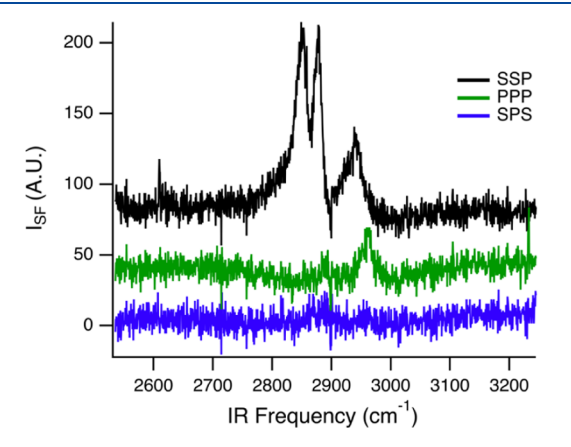


Figure 2. VSFG spectra of 100 mM trehalose in three polarization combinations.

shows the VSFG spectrum from the aqueous—vapor interface of a 100 mM Tre solution. The measurable VSFG signal shows Tre to be present at the surface, although independent surface tension measurements (not shown) indicate that Tre does not accumulate in excess. Provisional assignments can be made based on a combined density functional theory/FTIR study of anhydrous and partially hydrated trehalose²⁴ and SFG studies of molecules similar to trehalose.^{40,41} The peak at 2848 cm⁻¹ is assigned to a C—H vibration from the ring carbons.²⁴ The peaks at 2878 and 2940 cm⁻¹ are likely from a symmetric CH₂ stretch.^{40,41} The 2961 cm⁻¹ peak in the PPP-polarized spectrum is possibly a C—H stretch from a ring carbon influenced by an adjacent hydrogen bond to water²⁴ or an asymmetric CH₂ stretch.⁴¹

Figure 3 shows the VSFG spectra of DPPC monolayers at two different DPPC surface coverages, 55 and 40 Ų/molecule. These surface coverages correspond to a two-dimensional liquid condensed phase and a two-dimensional solid phase, respectively. The features at $\sim\!2870$ and $\sim\!2847~\text{cm}^{-1}$ correspond to the symmetric stretching modes of the DPPC methyl and methylene groups, respectively. Based on the literature assignments of Snyder et. al., these will also be referred to as the r^+ (methyl symmetric stretch) and d^+ (methylene symmetric stretch) peaks. 42

In the SSP-polarized data (top row), the SF intensity is a result of IR vibrational transition moments aligned perpendicular to the sample surface. In the expanded, $55 \text{ Å}^2/\text{molecule SSP}$ data (top left), the r⁺ peak is lower in intensity than the d⁺ peak with no and low Tre (0 and 1 mM) in the subphase. The low methyl

symmetric stretch intensity in comparison to a larger methylene symmetric stretch intensity implies a disorganized monolayer of DPPC molecules having disordered chains with gauche defects. As the Tre subphase concentration increases (10, 50, and 100 mM), the r⁺ intensity increases and exceeds that of the d⁺ band, indicating that the DPPC has become more conformationally ordered. In this context, conformationally ordered means lipid acyl chains having fewer gauche defects with more terminal methyl groups having their IR symmetric stretch vibrational transition moment normal to the surface versus methylene groups. A semiquantitative measure of alkyl chain organization in surfactant monolayer is often given by an r+/d+ intensity ratio. 12,43-45 These values are plotted in Figure 4. With the more expanded DPPC surface coverage (55 Å²/molecules), this ratio increases with increasing Tre subphase concentrations showing that increasing amounts of Tre in the subphase induce greater organization within the DPPC monolayer. This result is consistent with cooperative adsorption effects seen with other DPPC/monosaccharide interactions. 14,16 Although we see an increase in the r^+/d^+ ratio at the 55 Å²/molecule DPPC surface coverage, this ratio only reaches a value of 2.0, well below the upper limit of $\sim 5-7$ for the tightly packed lipid films (Figure

Under SPS polarization conditions, the IR field probes vibrations having their IR transition moments parallel to the surface. This polarization, with a surface coverage of 55 Å $^2/$ molecule (middle left), the VSG signal grows at $\sim\!2960~{\rm cm}^{-1}$ with increasing trehalose concentration in the subphase. This peak is assigned to a CH3 asymmetric stretch (r $^-$) and can result from structural and/or dynamic changes. For the spectra with lower concentrations of Tre, the r $^-$ would be expected to be larger for tilted and/or disordered DPPC monolayers than for ordered monolayers, but rapid internal motion of the methyl group about its C3 axis preferentially suppresses VSFG from r $^{-47}$ We propose that the growth of this peak with higher Tre concentrations results from Tre cooperatively adsorbing to the lipid headgroup and condensing the lipids to restrict methyl rotation.

In the PPP polarization combination, the moderately packed, $55 \, \text{Å}^2/\text{molecule DPPC}$ (left column, bottom) shows an increase in the r $^-$ peak intensity with Tre concentrations greater than 10 mM. This increase coincides with the flip in r $^+$ and d $^+$ intensities observed in the SSP-polarized data.

The left column of Figure 3 shows the spectra of DPPC at 40 Ų/molecule in SSP, SPS, and PPP polarization combinations. At this surface coverage, DPPC is tightly packed as a two-dimensional solid. In all polarization combinations, spectra show almost no variation as a function of Tre concentration. This behavior is attributed to the fact that DPPC at this coverage already has limited conformational mobility; so, any interactions between cooperatively adsorbed Tre and DPPC headgroups will not affect lipid chain organization. This assessment is supported by the $\rm r^+/d^+$ ratio (Figure 4) for the SSP-polarized spectra that show only modest changes with Tre concentration.

Tre's impact on monolayer behavior was examined further with π -area isotherms (Figure 5). The isotherms show little deviation from each other at 55 Ų/molecule at low Tre concentrations despite VSFG evidence that Tre is inducing conformational changes in monolayer organization. Only when the Tre concentration reaches 50 mM does the isotherm show explicit evidence of Tre-DPPC interaction. The π -area data from DPPC on a 50 mM Tre subphase is expanded with DPPC taking up a larger mean molecular area (MMA) at a given surface

The Journal of Physical Chemistry B

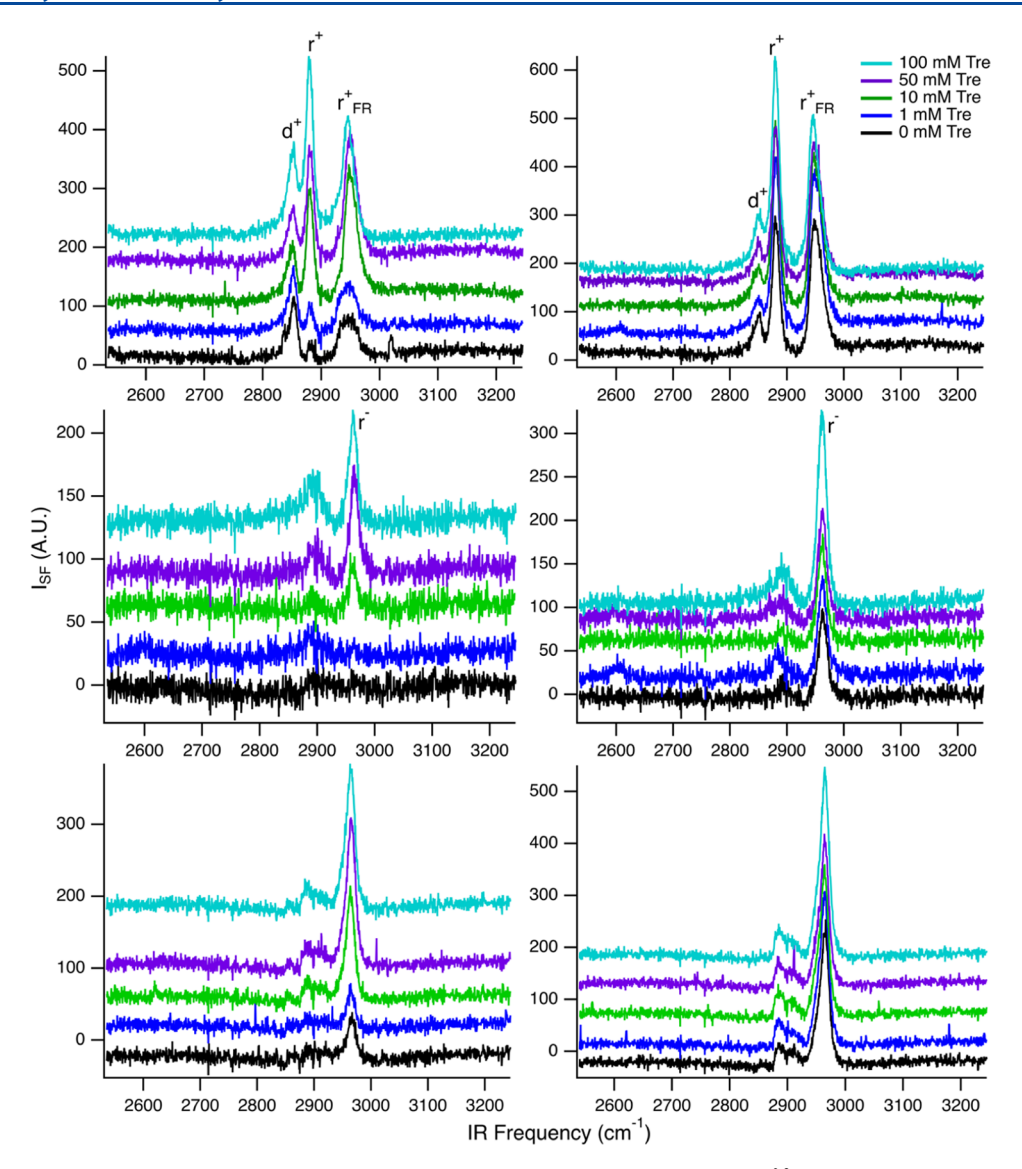


Figure 3. VSFG spectra of DPPC on different concentrations of Tre. The left column has DPPC at 55 $Å^2$ /molecule and the right at 40 $Å^2$ /molecule. The top row is in SSP polarization, the middle SPS, and the bottom PPP.

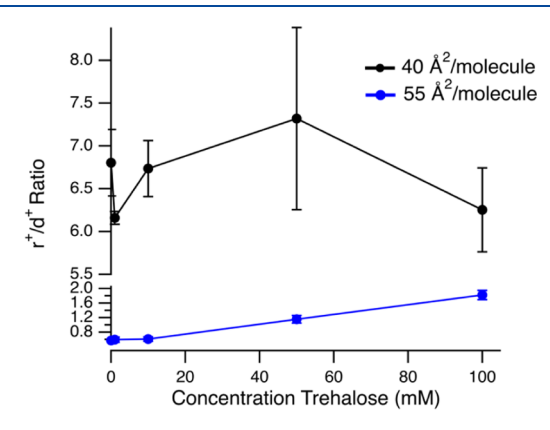


Figure 4. VSF r^+/d^+ intensity ratios for DPPC on Tre solutions. Data show the average results of 4 equiv measurements, and the error bars reflect one standard deviation uncertainty. Note that the anomalously large error bars for the 40 \mathring{A}^2 data with 50 mM trehalose in the subphase may have originated with temporary instrument inconsistencies. We do not attribute physical significance (such as binary phase formation, etc.) to this result.

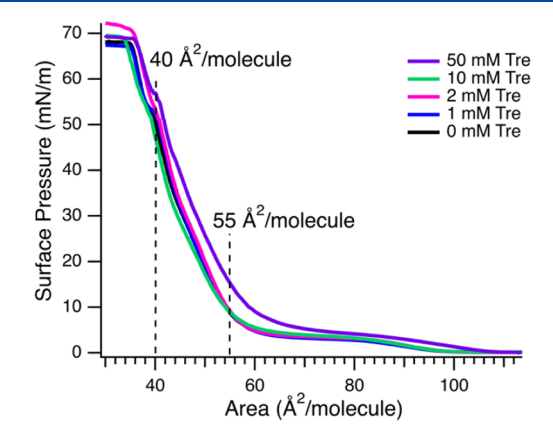


Figure 5. π –A isotherms of DPPC on trehalose solutions.

pressure. This increase can result from Tre integration into the monolayer causing a larger overall footprint (or MMA) for DPPC monomers.

Isotherm data were analyzed using excess free-energy expressions shown in eq 6. A negative excess free energy,

 $\Delta G^{\rm EX}$, in an ideal mixed monolayer with two surfactants restricted to the interface, indicates an attractive interaction between the two surface species, resulting in a more compressed monolayer that is a more stable monolayer of a single species.³⁸ In the case of trehalose and DPPC, trehalose is not constrained to the surface. With 50 mM Tre, excess free energy is positive (Figure 6). This behavior is the consequence of a more

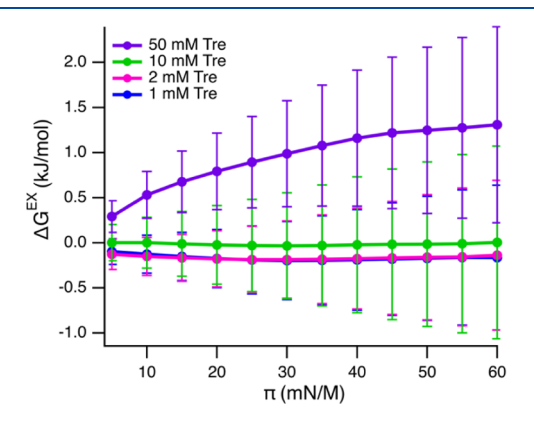


Figure 6. Excess free energy of mixing for DPPC on trehalose solutions.

expanded monolayer and also corresponds to a lower surface tension compared to pure DPPC at a given MMA. A decrease in surface tension can result from Tre displacing water and stabilizing the DPPC monolayer by forming more and/or stronger hydrogen bonds.

Taken together, SFG and surface tension data create a consistent story describing Tre's interactions with DPPC monolayers. Changes in SFG vibrational intensities for expanded monolayers show clear evidence of Tre-induced changes in monolayer structure and organization starting with 10 mM Tre. Surface tension data suggests that the Tre concentration threshold necessary to observe Tre-DPPC interactions is higher (50 mM); both surface tension and sum frequency data support a cooperative adsorption mechanism.

To further explore Tre cooperatively adsorbing to DPPC films, DSC measurements were performed using DPPC vesicles containing aqueous solutions with varying amounts of dissolved Tre. DSC data from solutions containing DPPC vesicles and different amounts of Tre are shown in Figure 7.

With 50 mM Tre, the overall endotherm peak shape is the same, but the peak has broadened to higher temperatures. This result shows that Tre interactions stabilize the DPPC membrane

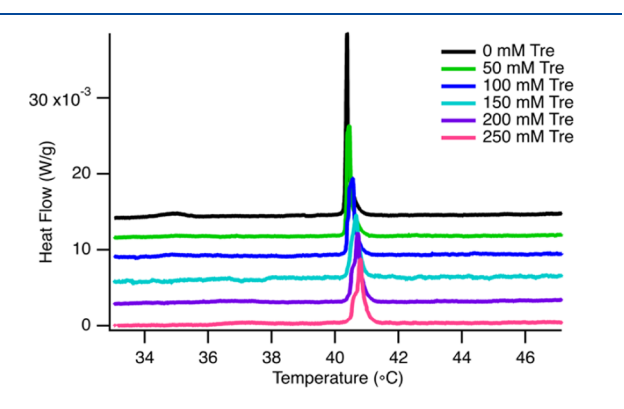


Figure 7. DSC measurements for DPPC vesicles in Tre solutions. All transitions are exothermic and offset for clarity.

and increase the energy needed to melt the bilayer. As the concentration of Tre increases further, the phase transition shifts to a higher temperature and a shoulder grows in at slightly lower temperatures. Other molecules that change lipid bilayer phase behavior in this way are proton translocators. 48 Proton translocators, such as picric acid and 2,4-dinitrophenol, are known to interact with lipid bilayers in a way to also produce a low-temperature shoulder relative to the parent transition peak. The similarities in the DSC data support a mechanism where Tre forms H-bonds with DPPC films.

CONCLUSIONS

Cooperative adsorption was investigated using the model system of DPPC monolayers deposited on aqueous solutions containing the neutral disaccharide trehalose. Nonlinear optical spectroscopy was used to probe C-H vibrations at the aqueous/ vapor interface from the DPPC monolayer. Using this technique, DPPC monolayers in their liquid condensed state showed increased organization when Tre was present in the aqueous subphase (for concentrations ≥ 10 mM Tre). Organization in more tightly packed DPPC data showed little change with Tre bulk concentration. In surface tension measurements, DPPC monolayer properties showed little effect from Tre until bulk concentrations reached 50 mM. Both measurements point to a Tre concentration threshold that must be reached cooperative adsorption affects lipid film structure. Future experiments are needed to narrow the concentration window and identify where cooperative adsorption begins to manifest and the specific origin of Tre-DPPC interactions. DSC measurements support a mechanism where hydrogen bonding between Tre and DPPC is the primary component of Tre's bioprotective mechanism.

ASSOCIATED CONTENT

Supporting Information

The Supporting Information is available free of charge on the ACS Publications website at DOI: 10.1021/acs.jpcb.9b07770.

VSFG spectra were acquired in the OH stretching region from DPPC monolayers at two different surface coverages on top of solutions containing different amounts of the disaccharide trehalose. Spectra were acquired under SSP polarization conditions using an EKSPLA spectrometer assembly. The data acquired with the scanning SFG system were not referenced to any external standard (PDF)

AUTHOR INFORMATION

Corresponding Author

*E-mail: rawalker@montana.edu.

Aashish Tuladhar: 0000-0003-2449-4984 Robert A. Walker: 0000-0002-0754-6298

The authors declare no competing financial interest.

ACKNOWLEDGMENTS

The material presented in this manuscript is based, in part, upon the work supported by the National Science Foundation EPSCoR Cooperative Agreement OIA-1757351. A portion of the research was performed using the William R. Wiley Environmental Molecular Science Laboratory (EMSL), a U.S.

Department of Energy's Office of Science User Facility sponsored by the Office of Biological and Environmental Research and located at Pacific Northwest National Laboratory (EMSL user proposal 49300). The authors also acknowledge support from the Montana Research and Economic Development Initiative (M-REDI). A.T. acknowledges support by the U.S. Department of Energy (DOE), Office of Science, Office of Basic Energy Sciences, Division of Materials Science and Engineering.

REFERENCES

- (1) Schiffer, J. M.; Mael, L. E.; Prather, K. A.; Amaro, R. E.; Grassian, V. H. Sea Spray Aerosol: Where Marine Biology Meets Atmospheric Chemistry. *ACS Cent. Sci.* **2018**, *4*, 1617–1623.
- (2) Clark, G. A.; Henderson, J. M.; Heffern, C.; Akgun, B.; Majewski, J.; Lee, K. Y. Synergistic Interactions of Sugars/Polyols and Monovalent Salts with Phospholipids Depend upon Sugar/Polyol Complexity and Anion Identity. *Langmuir* 2015, 31, 12688–12698.
- (3) Horta, B. A.; Peric-Hassler, L.; Hunenberger, P. H. Interaction of the Disaccharides Trehalose and Gentiobiose with Lipid Bilayers: A Comparative Molecular Dynamics Study. *J. Mol. Graphics Modell.* **2010**, 29, 331–346.
- (4) Pereira, C. S.; Hünenberger, P. H. The Influence of Polyhydroxylated Compounds on a Hydrated Phospholipid Bilayer: A Molecular Dynamics Study. *Mol. Simul.* **2008**, *34*, 403–420.
- (5) Frerking, I.; Gunther, A.; Seeger, W.; Pison, U. Pulmonary Surfactant: Functions, Abnormalities and Therapeutic Options. *Intensive Care Med.* **2001**, *27*, 1699–1717.
- (6) Pradhan, P.; Giri, J.; Rieken, F.; Koch, C.; Mykhaylyk, O.; Doblinger, M.; Banerjee, R.; Bahadur, D.; Plank, C. Targeted Temperature Sensitive Magnetic Liposomes for Thermo-Chemotherapy. *J. Controlled Release* **2010**, *142*, 108–121.
- (7) Andresen, T. L.; Davidsen, J.; Begtrup, M.; Mouritsen, O. G.; Jorgensen, K. Enzymatic Release of Antitumor Ether Lipids by Specific Phospholipase A2 Activation of Liposome-Forming Prodrugs. *J. Med. Chem.* **2004**, *47*, 1694–1703.
- (8) Zhao, Q.; Li, Y.; Chai, X.; Xu, L.; Zhang, L.; Ning, P.; Huang, J.; Tian, S. Interaction of Inhalable Volatile Organic Compounds and Pulmonary Surfactant: Potential Hazards of VOCs Exposure to Lung. *J. Hazard. Mater.* **2019**, 369, 512–520.
- (9) Bonn, M.; Roke, S.; Berg, O.; Juurlink; Stamouli, A.; Müller, M. A Molecular View of Cholesterol-Induced Condensation in a Lipid Monolayer. *J. Phys. Chem. B* **2004**, *108*, 19083–19085.
- (10) Ohe, C.; Sasaki, T.; Noi, M.; Goto, Y.; Itoh, K. Sum Frequency Generation Spectroscopic Study of the Condensation Effect of Cholesterol on a Lipid Monolayer. *Anal. Bioanal. Chem.* **2007**, 388, 73–79.
- (11) Adams, E. M.; Casper, C. B.; Allen, H. C. Effect of Cation Enrichment on Dipalmitoylphosphatidylcholine (DPPC) Monolayers at the Air-Water Interface. *J. Colloid Interface Sci.* **2016**, *478*, 353–364.
- (12) Adams, E. M.; Verreault, D.; Jayarathne, T.; Cochran, R. E.; Stone, E. A.; Allen, H. C. Surface Organization of a DPPC Monolayer on Concentrated SrCl2 and ZnCl2 Solutions. *Phys. Chem. Chem. Phys.* **2016**, *18*, 32345–32357.
- (13) Kučerka, N.; Dushanov, E.; Kholmurodov, K. T.; Katsaras, J.; Uhrikova, D. Calcium and Zinc Differentially Affect the Structure of Lipid Membranes. *Langmuir* **2017**, *33*, 3134–3141.
- (14) Link, K. A.; Hsieh, C.-Y.; Tuladhar, A.; Chase, Z.; Wang, Z.; Wang, H.; Walker, R. A. Vibrational Studies of Saccharide-Induced Lipid Film Reorganization at Aqueous/Air Interfaces. *Chem. Phys.* **2018**, *512*, 104–110.
- (15) Link, K. A.; Spurzem, G. N.; Tuladhar, A.; Chase, Z.; Wang, Z.; Wang, H.; Walker, R. A. Organic Enrichment at Aqueous Interfaces: Cooperative Adsorption of Glucuronic Acid to DPPC Monolayers Studied with Vibrational Sum Frequency Generation. *J. Phys. Chem. A* **2019**, *123*, 5621–5632.
- (16) Burrows, S. M.; Gobrogge, E.; Fu, L.; Link, K.; Elliott, S. M.; Wang, H.; Walker, R. OCEANFILMS-2: Representing Coadsorption of

- Saccharides in Marine Films and Potential Impacts on Modeled Marine Aerosol Chemistry. *Geophys. Res. Lett.* **2016**, *43*, 8306–8313.
- (17) Vipin, C.; Mujeeburahiman, M.; Arun, A. B.; Ashwini, P.; Mangesh, S. V.; Rekha, P. D. Adaptation and Diversification in Virulence Factors Among Urinary Catheter-Associated Pseudomonas Aeruginosa Isolates. *J. Appl. Microbiol.* **2019**, *126*, 641–650.
- (18) Crowe, L. M. Lessons from Nature: The Role of Sugars in Anhydrobiosis. *Comp. Biochem. Physiol., Part A: Mol. Integr. Physiol.* **2002**, *131*, 505–513.
- (19) Gil, A. M.; Belton, P. S.; Felix, V. Spectroscopic Studies of Solid α - α Trehalose. *Spectrochim. Acta, Part A* **1996**, *52*, 1649–1659.
- (20) Nagase, H.; Ueda, H.; Nakagaki, M. Effects of Sonication on the Lamellar Structures of L-Alpha-Dipalmitoyl Phosphatidylcholine-(DPPC)/Saccharide/Water Systems. *Chem. Pharm. Bull.* **1999**, 47, 1355–1362.
- (21) Ohtake, S.; Schebor, C.; de Pablo, J. J. Effects of Trehalose on the Phase Behavior of DPPC-Cholesterol Unilamellar Vesicles. *Biochim. Biophys. Acta, Biomembr.* **2006**, *1758*, 65–73.
- (22) Lenne, T.; Bryant, G.; Holcomb, R.; Koster, K. L. How Much Solute is Needed to Inhibit the Fluid to Gel Membrane Phase Transition at Low Hydration? *Biochim. Biophys. Acta, Biomembr.* **2007**, 1768, 1019–1022.
- (23) Luzardo, M. C.; Amalfa, F.; Nunez, A. M.; Diaz, S.; Biondi De Lopez, A. C.; Disalvo, E. A. Effect of Trehalose and Sucrose on the Hydration and Dipole Potential of Lipid Bilayers. *Biophys. J.* **2000**, *78*, 2452–2458.
- (24) Márquez, M. J.; Romani, D.; Díaz, S. B.; Brandán, S. A. Structural and Vibrational Characterization of Anhydrous and Dihydrated Species of Trehalose Based on the FTIR and FTRaman Spectra and DFT Calculations. J. King Saud Univ., Sci. 2018, 30, 229–249.
- (25) Crowe, L. M.; Crowe, J. H.; Chapman, D. Interaction of Carbohydrates with Dry Dipalmitoylphosphatidylcholine. *Arch. Biochem. Biophys.* **1985**, 236, 289–296.
- (26) Leekumjorn, S.; Sum, A. K. Molecular Dynamics Study on the Stabilization of Dehydrated Lipid Bilayers with Glucose and Trehalose. *J. Phys. Chem. B* **2008**, *112*, 10732–10740.
- (27) Venable, R. M.; Skibinsky, A.; Pastor, R. W. Constant Surface Tension Molecular Dynamics Simulations of Lipid Bilayers with Trehalose. *Mol. Simul.* **2006**, 32, 849–855.
- (28) Shultz, M. J.; Schnitzer, C.; Simonelli, D.; Baldelli, S. Sum Frequency Generation Spectroscopy of the Aqueous Interface: Ionic and Soluble Molecular Solutions. *Int. Rev. Phys. Chem.* **2000**, *19*, 123–153.
- (29) Ohno, P. E.; Wang, H. F.; Geiger, F. M. Second-Order Spectral Lineshapes from Charged Interfaces. *Nat. Commun.* **2017**, *8*, No. 1032.
- (30) Ohno, P. E.; Wang, H. F.; Paesani, F.; Skinner, J. L.; Geiger, F. M. Second-Order Vibrational Lineshapes from the Air/Water Interface. *J. Phys. Chem. A* **2018**, 122, 4457–4464.
- (31) Ohno, P. E.; Saslow, S. A.; Wang, H. F.; Geiger, F. M.; Eisenthal, K. B. Phase-Referenced Nonlinear Spectroscopy of the Alpha-Quartz/Water Interface. *Nat. Commun.* **2016**, *7*, No. 13587.
- (32) Gonella, G.; Lütgebaucks, C.; de Beer, A. G. F.; Roke, S. Second Harmonic and Sum-Frequency Generation from Aqueous Interfaces Is Modulated by Interference. *J. Phys. Chem. C* **2016**, *120*, 9165–9173.
- (33) Wen, Y.-C.; Zha, S.; Tian, C.; Shen, Y. R. Surface pH and Ion Affinity at the Alcohol-Monolayer/Water Interface Studied by Sum-Frequency Spectroscopy. *J. Phys. Chem. C* **2016**, *120*, 15224–15229.
- (34) Wen, Y. C.; Zha, S.; Liu, X.; Yang, S.; Guo, P.; Shi, G.; Fang, H.; Shen, Y. R.; Tian, C. Unveiling Microscopic Structures of Charged Water Interfaces by Surface-Specific Vibrational Spectroscopy. *Phys. Rev. Lett.* **2016**, *116*, No. 016101.
- (35) Doğangün, M.; Ohno, P. E.; Liang, D.; McGeachy, A. C.; Be, A. G.; Dalchand, N.; Li, T.; Cui, Q.; Geiger, F. M. Hydrogen-Bond Networks near Supported Lipid Bilayers from Vibrational Sum Frequency Generation Experiments and Atomistic Simulations. *J. Phys. Chem. B* **2018**, *122*, 4870–4879.
- (36) Reddy, S. K.; Thiraux, R.; Wellen Rudd, B. A.; Lin, L.; Adel, T.; Joutsuka, T.; Geiger, F. M.; Allen, H. C.; Morita, A.; Paesani, F. Bulk

Contributions Modulate the Sum-Frequency Generation Spectra of Water on Model Sea-Spray Aerosols. *Chem* **2018**, *4*, 1629–1644.

- (37) Blume, A. Lipids at the Air-Water Interface. ChemTexts 2018, 4, 3.
- (38) Gzyl-Malcher, B.; Paluch, M. Studies of Lipid Interactions in Mixed Langmuir Monolayers. *Thin Solid Films* **2008**, *516*, 8865–8872.
- (39) Gobrogge, C. A.; Kong, V. A.; Walker, R. A. Temperature-Dependent Partitioning of C152 in Binary Phosphatidylcholine Membranes and Mixed Phosphatidylcholine/Phosphatidylethanolamine Membranes. *J. Phys. Chem. B* **2017**, *121*, 7889–7898.
- (40) Zhang, L.; Fu, L.; Wang, H.-f.; Yang, B. Discovery of Cellulose Surface Layer Conformation by Nonlinear Vibrational Spectroscopy. *Sci. Rep.* **2017**, *7*, No. 44319.
- (41) Hieu, H. C.; Li, H.; Miyauchi, Y.; Mizutani, G.; Fujita, N.; Nakamura, Y. Wetting Effect on Optical Sum Frequency Generation (SFG) Spectra of D-Glucose, D-Fructose, and Sucrose. *Spectrochim. Acta, Part A* **2015**, *138*, 834–839.
- (42) MacPhail, R. A.; Strauss, H. L.; Snyder, R. G.; Elliger, C. A. Carbon-Hydrogen Stretching Modes and the Structure of n-Alkyl Chains. 2. Long, All-Trans Chains. *J. Phys. Chem. A* **1984**, 88, 334–341.
- (43) Can, S. Z.; Mago, D. D.; Walker, R. A. Structure and Organization of Hexadecanol Isomers Adsorbed to the Air/Water Interface. *Langmuir* **2006**, 22, 8043–8049.
- (44) Walker, R. A.; Gruetzmacher, J. A.; Richmond, G. L. Phosphatidylcholine Monolayer Structure at a Liquid-Liquid Interface. J. Am. Chem. Soc. 1998, 120, 6991-7003.
- (45) Conboy, J. C.; Messmer, M. C.; Richmond, G. L. Dependence of Alkyl Chain Conformation of Simple Ionic Surfactants on Head Group Functionality As Studied by Vibrational Sum-Frequency Spectroscopy. *J. Phys. Chem. B* **1997**, *101*, 6724–6733.
- (46) Walker, R. A.; Gruetzmacher, J. A.; Richmond, G. L. Phosphatidylcholine Monolayer Structure at a Liquid-Liquid Interface. J. Am. Chem. Soc. 1998, 120, 6991-7003.
- (47) Fourkas, J. T.; Walker, R. A.; Can, S. Z.; Gershgoren, E. Effects of Reorientation in Vibrational Sum-Frequency Spectroscopy. *J. Phys. Chem. C* **2007**, *111*, 8902–8915.
- (48) Jain, M. K.; Wu, N. M. Effect of Small Molecules on the Dipalmitoyl Lecithin Liposomal Bilayer: III. Phase Transition in Lipid Bilayer. *J. Membr. Biol.* **1977**, 34, 157–201.